Bocconi

WORKING PAPER SERIES
ISSN 2785-1079

Number 12
DECEMBER 2020

RESILIENCE TO HEALTH SHOCKS AND THE SPATIAL EXTENT OF LOCAL LABOUR MARKETS: EVIDENCE FROM THE COVID-19 OUTBREAK IN ITALY

Mattia Borsati

Michele Cascarano

Marco Percoco

Università Bocconi
GREEN
Centre for Geography, Resources, Environment, Energy and Networks

Resilience to health shocks and the spatial extent of local labour markets: evidence from the COVID-19 outbreak in Italy

Mattia Borsati[a], Michele Cascarano[b], Marco Percoco[a]

[a] *Dept. of Social and Political Sciences and GREEN, Bocconi University, Milan, Italy*
[b] *Economic Research Unit, Bank of Italy, Trento, Italy*

Abstract

SARS-CoV-2 uses human beings as means of transport. In addition to the general issue that fewer interpersonal contacts reduce the speed of contagion, less attention has been paid to the spatial configuration of such contacts. With respect to Italy, the virus severely affected the most industrialized area of the country, where the high density of economic activities also exhibits dense networks of commuting flows. In this article, we empirically investigate the relationship between the spatial extent of local labour markets, as defined by the structure of the commuting network, and the diffusion of COVID-19. To this end, we compute, for each municipality, the intensive and extensive margins of commuting flows and we measure the spread of the disease by considering excess mortality over the period of January-May 2020. By exploiting a rich and novel dataset, we find that the commuting network played a significant role in placing more connected places at more severe epidemiological risk. A back-of-the-envelope calculation suggests that if commuting patterns were 90% of the real ones, Italy would have suffered approximately 1 300 and 1 000 fewer fatalities in March and April, respectively.

Keywords: COVID-19, Resilience, Local labour market, Commuting flows, Mobility

JEL Classification Numbers: H12, I18, J61, R41

---

1. Introduction

The daily mobility of individuals for motives of labour is one of the main features of developed societies, so the spatial extent of local labour markets is in fact defined on the basis of the geography of commuting flows. The openness of such areas generates costs and benefits for the governance of the local economy, particularly in the case of a pandemic. In this article, we investigate how the openness of local labour markets, as defined by the structure of the commuting network, influences the resilience of cities to health shocks, such as the COVID-19 outbreak. In particular, we explore the aforementioned dynamics in Italy, the first Western country to be deeply affected by the disease.

Email addresses: `mattia.borsati@unibocconi.it` (Mattia Borsati), `michele.cascarano@bancaditalia.it` (Michele Cascarano), `marco.percoco@unibocconi.it` (Marco Percoco)

December 2020

There are several reasons why we believe that such an empirical analysis is needed for a thorough comprehension of the phenomenon. First, the virus spread across Italy first and foremost in the most industrialized area of the country, suggesting a possible correlation between the structural features of local economies and the epidemic. Second, places characterized by high density of economic activities also exhibit dense networks of spatial interactions (especially in the form of commuting flows), and these flows in their turn place such places at more severe epidemiological risk, as shown by other epidemics (Zhou et al., 2019). In fact, Bergamo, the city among the provincial capitals with the largest share of incoming and outgoing workers compared to the population overall, is the one that also experienced the greatest increase in fatalities recorded in March 2020 (+429%), compared to the 2015-2019 average. Not surprisingly, the openness of Bergamo's labour market is remarkable because it is the epicentre of the largest industrial district in the whole nation[1]

In response to the diffusion of Covid-19, several national governments imposed unprecedented lockdown restrictions to slow the infection rate and save lives (Greenstone and Nigam, 2020). Indeed, in the absence of medical treatments, such as vaccines or pharmaceuticals, the limitation of interpersonal contacts is a key policy for containing viral infections (Haushofer and Metcalf, 2020; Van Bavel et al., 2020). As a result, the travel behaviours of people have been drastically altered (De Vos, 2020), with dramatic economic and social consequences (Bonaccorsi et al., 2020).

With the aim of understanding the efficiency of social distancing measures, several studies have started to analyse the mobility patterns of people during the emergency (e.g., Beria and Lunkar, 2020), as well as the impact of cultural norms on citizens' compliance with such extreme rules in different countries, such as Italy (Durante et al., 2020), Sweden (Born et al., 2020), several other European countries (Bartscher et al., 2020), and the United States (Borgonovi and Andrieu, 2020). With respect to other studies shedding light on the role of actual mobility on the spread of contagion (e.g., Fang et al., 2020; Monte, 2020), we differ substantially by focusing on the relationship between the structure of the network of commuting flows and the initial diffusion of the disease. To the best of our knowledge, this article is the first attempting to address this specific issue. To this end, we analyse commuting patterns at the municipality level using data from the latest official country-wide assessment of mobility for Italy. Similarly, we measure the spread of COVID-19 by considering excess mortality over the period of January-May 2020, comprising several weeks both before and after the most critical part of the pandemic cycle. We also consider a broad set of additional municipality characteristics to control for other specific dynamics (see Section 3 for further details on the variable construction process and data sources). After assembling the novel dataset, our empirical strategy exploits within-municipality

[1] Industrial districts are "self-contained" labour markets mainly consisting of small- and medium-sized enterprises specializing in the same economic activity. According to the latest industry and services national census, the industrial district of Bergamo is the largest in terms of population (802 731) and embedded municipalities (123).

variation in excess mortality over time by estimating a two-way fixed effects model in which all of our explanatory variables are interacted with month dummies.

Our article provides some relevant novelties in two directions: first, we examine the structure of the commuting network by computing both the intensive and extensive margins of commuting flows; and second, we exploit more granular and heterogeneous data by performing the analysis at the municipality level, while most of the previous studies focused on main cities (Glaeser et al., 2020), provinces (Iacus et al., 2020), or regions (Cintia et al., 2020).

More precisely, we compute two synthetic indices that describe commuting flows under different perspectives: the intensity of external mobility and the centrality of each municipality. The first index - the intensive margin - is defined as the total number of workers moving from and to a municipality over its population, similar to what is proposed by Murgante et al. (2020). In other words, it is a proxy for the share of the population exposed to the possibility of the virus being imported from elsewhere. The second index - the extensive margin - is based on the topological concept of relative degree centrality of a node within a network, measuring the importance and the openness of a municipality, as defined by Patuelli et al. (2009, 2010). In other words, the aim is to measure the number of other different places (each of which may have a different infection rate) to which the municipality is connected.

Our findings suggest that the spatial extent of local labour markets played a crucial role in influencing the resilience of cities to the COVID-19 shock. In particular, a 1 percentage point increase in the intensive margin is associated, on average, with 1.43 and 0.91 percentage point increases in excess mortality in March and April, respectively, while the same increase in the extensive margin is associated with a 3.44 increase in our outcome of interest in April. As a result, more isolated and less central places are found to be more resilient than others.

The remainder of the article is organized as follows. Section 2 briefly summarizes the timeline of the COVID-19 crisis in Italy. Section 3 describes the data used in the analysis. Section 4 discusses the empirical strategy and our main results. Section 5 concludes the study.

2. COVID-19 in Italy

Our empirical analysis focuses on Italy, the first Western country that was forced to shut down its economy to "flatten the curve" and contain the diffusion of COVID-19. Therefore, Italy represents the ideal scenario for investigating the relationship between commuting flows and the diffusion of the virus because government and citizens were unprepared to face the pandemic, while both policymakers and populations of other European countries have been influenced by the Italian case. Such an unfortunate situation limits the number of confounding factors because there were no countermeasures or policy responses during the first weeks of the outbreak.

The timeline of the main events is the following. The first two COVID-19 cases in Italy were officially detected on January 30, after a Chinese couple travelled from Wuhan to Milan, Verona, Parma, and Florence. The first cases of secondary transmission were identified near Codogno and Vo' (two municipalities in the Lombardy and Veneto regions, respectively) on

February 21, and two days later, the Italian government enforced mobility restrictions into and from these areas (DPCM1, 2020). On March 4, all schools and universities were closed (DPCM2, 2020). On March 8, the lockdown was imposed for the first relevant "red zone" of the country (DPCM3, 2020), that is, the whole Lombardy region and 14 additional provinces within the Emilia-Romagna, Marche, Piedmont, and Veneto regions[2] (see Figure B.1 for a detailed map). On March 11, the lockdown was extended to the whole nation (DPCM4, 2020), and many business activities open to the public were forced to close. Between March 22 and March 25, the "economic" lockdown was tightened further by shutting down all non-essential economic activities and prohibiting any movement of people on Italian soil with few exceptions, such as for work or health reasons (DPCM5, 2020; DPCM6, 2020). This step marked the so called "phase 1" of the epidemic, which gradually ended between May 4 and May 18.

3. Data

To study the spatial diffusion of the recent COVID-19 pandemic, we rely on two main data sources: the *Italian National Institute of Statistics* (ISTAT) and the *Italian Institute for Environmental Protection and Research* (ISPRA). In the following section we describe the variables used in the empirical analysis.

3.1. Measuring resilience through excess mortality

For 7 357 Italian municipalities out of 7 904 (covering approximately 95% of the total population), we obtain data released by ISTAT on July 9, 2020, that is, the monthly number of fatalities occurring during the first five months of 2020 and the average monthly number of fatalities occurring during the same period in 2015-2019. For the sake of simplicity, we refer to the latter data as the "baseline" throughout the rest of the article. Then, our outcome of interest is *mortality_growth*, defined as the increase in fatalities recorded in January, February, March, April and May 2020 compared to the same period in the "baseline"[3]:

$$mortality\_growth_{it} = \frac{fatalities_{it}^{2020} - fatalities_{it}^{baseline}}{fatalities_{it}^{baseline}} \quad (1)$$

This measure of the incidence of COVID-19 is directly related to the notion of local resilience (Boschma, 2015) since it computes the burden of the disease as a deviation from a pre-existing trend. We consider excess mortality our main outcome of interest over the official number of COVID-19 cases because it allows us to overcome, at least partially, major measurement errors and endogeneity issues related to the number of reported cases, such as non-random differences in screening procedures and testing capacity among areas. Indeed, it allows us to observe any

[2]The 14 additional provinces that completed the containment areas are Modena, Parma, Piacenza, Reggio nell'Emilia, Rimini, Pesaro e Urbino, Alessandria, Asti, Novara, Verbano-Cusio-Ossola, Vercelli, Padova, Treviso, and Venezia

[3]The evolution of excess mortality in Italy during the period of analysis is plotted in Figure D.1.

COVID-19-related fatalities, even before February 21, when the first Italian COVID-19 hotspots were identified[4]. Similarly, we prefer total fatalities over official COVID-19 fatalities because the latter are no longer considered a reliable measure due to differences in classification among hospitals (Buonanno et al., 2020). Moreover, it is plausible to expect that the official numbers are underestimating the true increase in mortality since a substantial number of people died without being tested (Ciminelli and Garcia-Mandicó, 2020; Bartoszek et al., 2020). Indeed, during the first quarter of 2020, Italy experienced 46 909 more deaths with respect to the average number of fatalities occurring in the same period during 2015-2019, while the official COVID-19 fatalities declared by the Department of Civil Protection numbered 27 938 (INPS, 2020). Hence, it is likely that the majority of the remaining 18 971 fatalities were also caused by the pandemic[5]. In addition, the use of such measures also allows us to consider the indirect effects of the pandemic, such as the possible increase in fatalities caused by other diseases that were not treated as usual due to hospital congestion.

3.2. Measuring the spatial extent of local labour markets

The aim of this article is to investigate the role played by the spatial extent of local labour markets in influencing their resilience to the spread of COVID-19. To this end, we use data on the network of commuting flows reported in the 2011 census in the form of a nationwide origin-destination matrix. We measure the intensity of external mobility of each municipality by considering both the out-flows, indicating the total number of workers w_{ij} moving from their residential municipality i to any other municipality $j = 1 \ldots n$ (excluding j = i), and the in-flows, indicating the total number of workers w_{ji} moving to municipality i from any other municipality j. We compute, for each municipality, the intensive margin of commuting, defined as the sum of the incoming and outgoing flows over the 2011 population of the area:

$$intensive\_margin_i = \frac{\sum_{j=1}^{n}(w_{ij} + w_{ji})}{population_i} \tag{2}$$

We also consider a topological index. We first compute the total number of direct inward and outward connections of each municipality (*degree_centrality*), that is, the set of origin-destination routes used by at least one worker to commute. Then, we define the extensive margin of commuting as the ratio between the observed and the maximum possible number of connections of a municipality:

$$extensive\_margin_i = \frac{degree\_centrality_i}{n - 1} \tag{3}$$

[4]By analysing the first three complete genomes of SARS-CoV-2, Zehender et al. (2020) showed that the virus was present in Italy weeks before the first reported case.

[5]During the period of May 25–July 15 2020, the Italian Ministry of Health and ISTAT conducted an epidemiological investigation to estimate the percentage of the population that likely contracted the infection by sampling 150 000 individuals throughout the whole Italian territory. The results (based on 64 660 serological tests) show that the number of people who contracted the virus is equal to 2.5% of the population and therefore 6 times more than the official COVID-19 cases detected over the pandemic cycle (ISTAT, 2020).

3.3. Control variables

To separate the effect of commuting flows from other confounding factors, we consider another important dimension linked to the movement of people, such as internal mobility. To this end - and by relying on the same 2011 census - we compute an $internal\_mobility$ index as the ratio of self-flows, indicating the total number of workers w_{ii} moving within their residential municipality i to reach the workplace, to the 2011 population of the area.

Then, we further control for other variables potentially correlated with both excess mortality and commuting patterns. In particular, we add all those predictors that are essential in standard epidemiological models to explain the spatial diffusion of a disease (e.g., Bisin and Moro, 2020; Desmet and Wacziarg, 2020). Hence, we first capture relevant geographic and demographic characteristics by including two dummy variables that take the value of 1 if a municipality is located near the sea (*coastal*) or at medium-high altitude (*mountainous*) and 0 otherwise, the log of the population density ($ln\_density$), and a proxy of physical proximity, defined as the log of the average number of square metres per inhabitant in occupied dwellings ($ln\_house\_m^2\_pc$).

Second, given that the fatality rates for males are two to three times higher than for females (Porcheddu et al., 2020), that the fatality rate is positively correlated with a larger presence of elderly people (Knittel and Ozaltun, 2020), that nursing homes and hospitals were the locations of the first outbreaks of the pandemic (Alacevich et al., 2020; Barnett and Grabowski, 2020), and that pollution can be an important co-determinant of COVID-19-related fatalities in northern Italy[6] (Becchetti et al., 2020; Coker et al., 2020; Conticini et al., 2020), we also control for five measures of vulnerability to the pandemic: the share of male population at the municipality level ($share\_males$), the share of population older than 75 years old at the municipality level ($share\_over75$), the share of individuals older than 65 years old cohabiting with younger individuals at the municipality level ($share\_cohab\_over65$), the number of hospital beds per capita at the province level ($hospital\_beds\_pc$), and the PM10, defined as the average values of μg/m^3 at the province level ($pm10$).

Third, we account for differences in economic structure between areas by including a dummy variable that takes the value of 1 if a municipality is located within an industrial district (*district*) and 0 otherwise. Indeed, the related literature shows how work-related mobility within industrial clusters is very high (OECD, 2002), as well as how these areas foster higher levels of social interactions (Gordon and McCann, 2000; Majocchi and Presutti, 2009). Finally, we have seen how the pandemic has induced many workers to perform their duties from home, preventing them from traveling. Thus, it might be that municipalities with larger numbers of "remote" workers experienced fewer COVID-19-related fatalities with respect to others. To capture this possible dynamic, we compute a working remotely index ($remote\_working$) by weighting the set of working remotely indices provided by Barbieri et al. (2020) by the labour force composition

[6]Several studies in the medical literature have shown that individuals living in highly polluted areas have a reduced capacity to react to respiratory diseases and pneumonias (Pope III and Dockery, 2006).

of each municipality (as defined by the 1-digit ATECO[7] sections).

All of the data are publicly available[8]. Table C.1 reports standard descriptive statistics of the variables used in the empirical analysis, as well as their reference year.

3.4. Descriptive evidence

In this section we briefly describe the spatial patterns of our main variables of interest. Figure 1 plots the spatial evolution of *mortality_growth* in March 2020, i.e., when Italy was severely affected by the pandemic (see Figure D.2 for the same map in the other months). Clearly, we can note how COVID-19-related fatalities appear to be spatially clustered in the northern part of Italy, particularly in the Lombardy region and across the Po Valley area[9]. Overall, the virus spread first and foremost in the most industrialized area of the country, suggesting a possible correlation between the structural features of local economies, such as the spatial interactions of workers, and the epidemic. As we can see in Figures 2 and 3, this area also shows high density of commuting flows, both in the intensive and the extensive components[10]. The visual correlation, especially between excess mortality and the intensity of external mobility, is striking and suggests a specific role of commuting flows in placing more connected places at more severe epidemiological risks.

4. Empirical analysis

4.1. Econometric model

To examine the relationship between the characteristics of commuting flows and excess mortality, we estimate the following equation:

$$\begin{aligned} mortality\_growth_{it} = \beta_0 + \beta_t intensive\_margin_i \times \delta_t + \gamma_t extensive\_margin_i \times \delta_t \\ + \eta_t Z_i \times \delta_t + \alpha_i + \delta_t + \epsilon_{it} \end{aligned} \tag{4}$$

[7] The ATECO 2007 classification is the Italian equivalent of the European NACE Rev. 2 classification.

[8] *mortality_growth* data are retrieved from https://www.istat.it/it/archivio/240401. *intensive_margin*, *extensive_margin*, and *internal_mobility* data are retrieved from https://www.istat.it/it/archivio/157423. *coastal*, *mountainous*, and *ln_density* data are retrieved from https://www.istat.it/it/archivio/156224. $ln\_house\_m^2\_pc$, $share\_over75$, and $share\_cohab\_over65$ data are retrieved from http://ottomilacensus.istat.it/. *share_males* and *hospital_beds_pc* data are retrieved from http://dati.istat.it/. $pm10$ data are retrieved from https://www.isprambiente.gov.it/it/pubblicazioni/stato-dellambiente/xiv-rapporto-qualita-dell2019ambiente-urbano-edizione-2018. *district* data are retrieved from https://www.istat.it/it/archivio/150320. *remote_working* data are retrieved from http://dati-censimentoindustriaeservizi.istat.it/Index.aspx and Barbieri et al. (2020).

[9] Nevertheless, by relying on a spatial weights matrix constructed through Euclidean distances without neighbourless municipalities, the Moran's I index for spatial autocorrelation of our outcome of interest is relatively low (0.13).

[10] Additional maps for the main control variables are provided in Figure D.3.

Figure 1: *mortality_growth* in March, by municipality

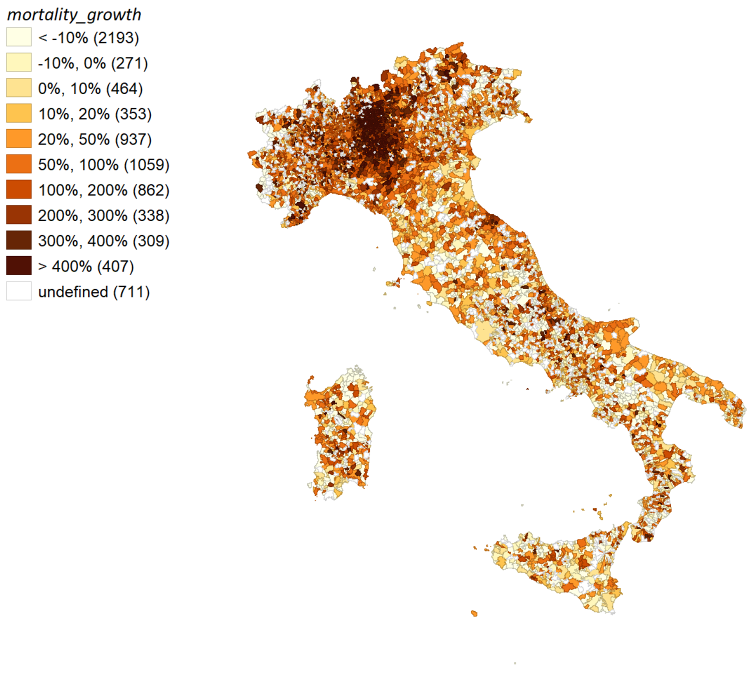

Source: Authors' own elaboration

Figure 2: *intensive_margin*, by municipality

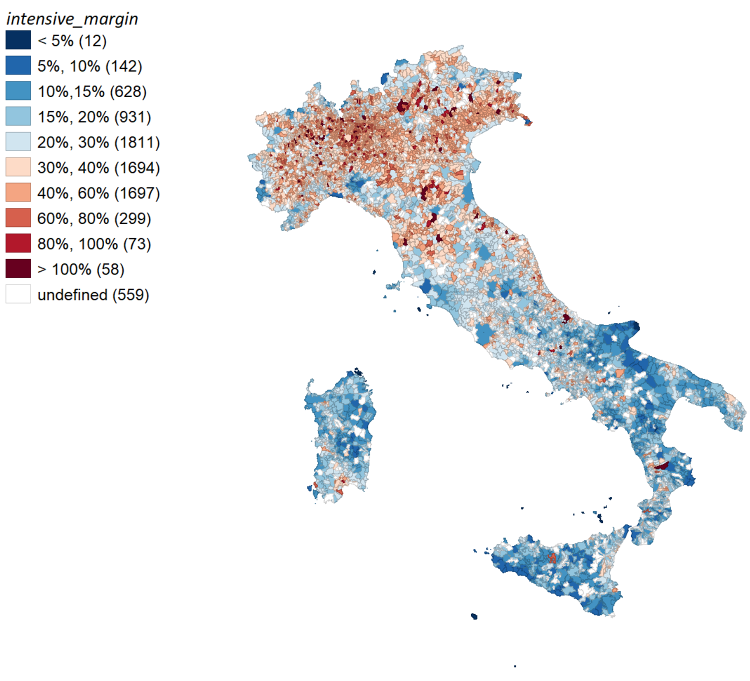

Source: Authors' own elaboration

Figure 3: *extensive_margin*, by municipality

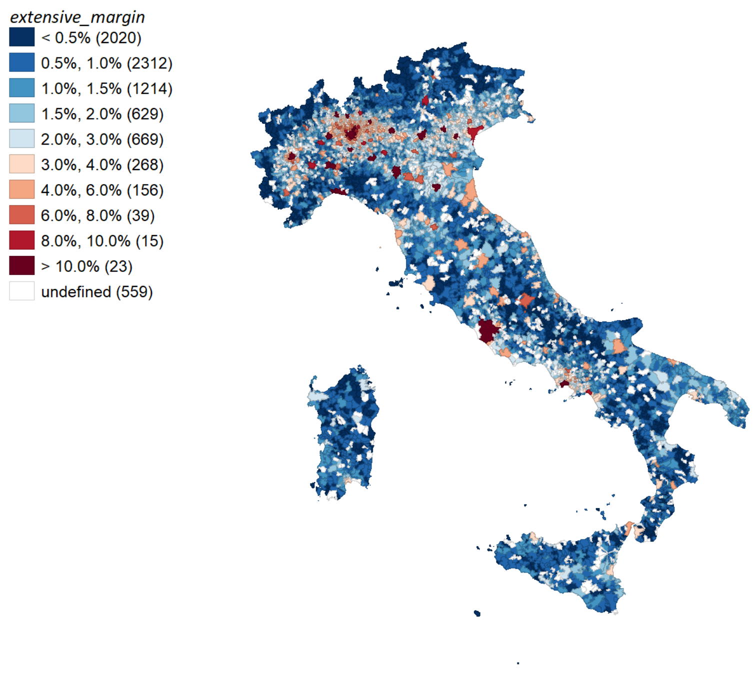

Source: Authors' own elaboration

where $mortality\_growth_{it}$ measures the increase in fatalities occurring in municipality i in month t, compared to the same period at "baseline". On the right-hand side, $intensive\_margin_i$ and $extensive\_margin_i$ are our municipality commuting indices interacted with a vector of monthly specific fixed effects, δ_t, accounting for the nationwide common evolution of excess mortality in a given month, such as the seasonal trend. By excluding January as the pre-outbreak period, the vectors of coefficients β_t and γ_t capture the impact of the structural characteristics of commuting flows on excess mortality over the various months of the pandemic cycle. $Z_i \times \delta_t$ indicates the internal mobility, geographic, demographic, vulnerability, and economic controls, also interacted with month dummies. Then, α_i is a full set of municipality-level fixed effects intended to absorb any difference in excess mortality due to time-invariant characteristics. Hence, by controlling for all of these observed and unobserved characteristics, our identifying assumption is that no other factor correlated with workers commuting systematically affects excess mortality. Finally, given that the geography of commuting flows analysed in this article essentially describes the spatial extent of local labour markets (Kropp and Schwengler, 2016), ϵ_{it} are heteroskedasticity- and autocorrelation-consistent standard errors, respectively clustered at the local labour market (LLM) level.

4.2. Estimation results

Tables 1 and 2 report regression results for Equation 4. The rationale for the structure of the two tables is to progressively include fixed effects and control variables to test the strength of our estimates.

In Table 1, the first two columns report the estimated coefficients for the specifications in which the intensive and extensive margins, interacted with month dummies, are included one at a time. Accordingly, the main effects of the interactions are included as well. In column 3, the two margins are simultaneously estimated, while in column 4, the specification adds a full set of region fixed effects because the Italian national health system is managed at the regional level. Finally, column 5 substitutes the region fixed effects with a full set of municipality fixed effects to better control for time-invariant characteristics of each observation potentially correlated with both excess mortality and commuting flows[11]. Overall, almost all of the estimated coefficients of the two margins preserve their signs and significance throughout the columns, their magnitudes decreasing as the specifications become less parsimonious.

In Table 2 we report estimates of regressions in which we have extended the set of controls. Interestingly, the estimated coefficients of the two margins remain consistent as, moving from the most parsimonious specification in column 1 to the most extended in column 4, their magnitude decreases without leading to a substantial increase in the standard error. Thus, our estimates suggest an important role played by the spatial extent of local labour markets in influencing the resilience of municipalities during the COVID-19 outbreak. Indeed, the intensity of external mobility - the intensive margin - and the topological centrality of a municipality - the extensive margin - are positively correlated with excess mortality during the most critical part of the pandemic. This empirical evidence suggests how greater connectivity renders places less resilient to epidemic health shocks.

For simplicity, we discuss further only the estimates in column 4 because they are obtained with the most complete specification in relation to our data. Given that January is our reference period, regression results are close to zero and not statistically significant in February, that is, when the COVID-19 virus had just begun to spread. As expected, the *intensive_margin* shows its strongest correlation with excess mortality in March, when Italy was suddenly and severely affected by the pandemic. The coefficient indicates that, holding constant the other variables, a 1 percentage point increase in the share of population moving from and to a municipality is associated, on average, with a 1.43 percentage point increase in excess mortality. Then, following the introduction of all of the containment measures described in Section 2, this positive correlation remain significant in April but with a smaller magnitude (0.91), while it loses significance and approaches zero in May. The *extensive_margin*, instead, shows its statistically significant correlation only in April, likely because the most central nodes of the commuting

[11] Given that our *intensive_margin* and *extensive_margin* are time-invariant variables, they are omitted from column 5 because of collinearity with municipality fixed effects.

Table 1: Commuting indices and mortality growth (part 1)

	mortality_growth				
	(1)	(2)	(3)	(4)	(5)
intensive_margin × *February*	0.024		0.054	0.067	0.078
	(0.085)		(0.089)	(0.088)	(0.090)
intensive_margin × *March*	2.326***		2.053***	2.050***	2.070***
	(0.442)		(0.342)	(0.342)	(0.341)
intensive_margin × *April*	1.304***		1.178***	1.175***	1.191***
	(0.148)		(0.156)	(0.155)	(0.158)
intensive_margin × *May*	0.137		0.133	0.128	0.157*
	(0.085)		(0.088)	(0.088)	(0.089)
extensive_margin × *February*		-1.122	-1.365*	-1.475*	-1.424*
		(0.806)	(0.824)	(0.820)	(0.826)
extensive_margin × *March*		21.020**	11.770*	11.760	11.750
		(8.515)	(7.141)	(7.142)	(7.150)
extensive_margin × *April*		10.720***	5.434***	5.446***	5.380***
		(1.713)	(1.497)	(1.500)	(1.484)
extensive_margin × *May*		0.779	0.183	0.141	0.146
		(0.878)	(0.885)	(0.885)	(0.879)
intensive_margin	0.055		0.074	-0.441***	
	(0.049)		(0.051)	(0.081)	
extensive_margin		-0.519	-0.854	-5.551***	
		(0.579)	(0.583)	(1.238)	
constant	-0.052**	-0.027	-0.048**	0.143***	-0.033
	(0.022)	(0.018)	(0.023)	(0.045)	(0.025)
Month FE	✓	✓	✓	✓	✓
Region FE	×	×	×	✓	×
Municipality FE	×	×	×	×	✓
Observations	35 916	35 916	35 916	35 916	35 916
R^2	0.07	0.06	0.07	0.10	0.08

Notes: All of the specifications present OLS estimates and include month, region, and municipality fixed effects as indicated. Standard errors clustered at the LLM level appear in parentheses. Significance values: ***p<0.01, **p<0.05, *p<0.10.

network played a pivotal role in spreading the disease later. The coefficient indicates that a 1 percentage point increase in the ratio between the observed and the maximum possible number of connections of a municipality is associated, on average, with a 3.44 percentage point increase in our outcome of interest, all else being equal[12].

That said, we provide some back-of-the-envelope calculations by considering three scenarios in which the intensive margins among Italian municipalities would be equal to 90%, 80%, and 70% of those actually observed in our data. In other words, we are interested in understanding what the average reduction in *mortality_growth* would have been had commuting flows been lower. For each scenario, Figure 4 shows these reductions for the months in which our *intensive_margin* coefficients are strongly significant. By focusing on the mildest scenario[13],

[12]For the sake of completeness, estimates of all of the control variables are reported in Table C.2, while Figure D.4 plots the coefficients of the most complete specification of Table 2 with their 95% and 99% confidence intervals.

[13]By way of example, this scenario would correspond to the situation in which the city of Bergamo, the provincial capital with both the highest *intensive_margin* and *mortality_growth* in March (as discussed in

Table 2: Commuting indices and mortality growth (part 2)

	mortality_growth			
	(1)	(2)	(3)	(4)
$intensive\_margin \times February$	0.114	0.120	0.096	0.098
	(0.095)	(0.102)	(0.103)	(0.108)
$intensive\_margin \times March$	1.896***	1.804***	1.430***	1.427***
	(0.299)	(0.292)	(0.285)	(0.277)
$intensive\_margin \times April$	1.141***	1.034***	0.882***	0.906***
	(0.170)	(0.173)	(0.166)	(0.162)
$intensive\_margin \times May$	0.153	0.107	0.095	0.095
	(0.094)	(0.099)	(0.104)	(0.108)
$extensive\_margin \times February$	-1.881**	-0.698	-0.748	-0.771
	(0.891)	(1.075)	(1.086)	(1.093)
$extensive\_margin \times March$	14.000	11.820	6.064	8.556
	(8.531)	(7.995)	(6.930)	(6.596)
$extensive\_margin \times April$	6.032***	6.263***	2.643*	3.442**
	(1.767)	(1.680)	(1.567)	(1.590)
$extensive\_margin \times May$	0.198	-0.405	-1.352	-1.620
	(0.926)	(1.026)	(1.054)	(1.109)
constant	-0.034	-0.034	-0.034	-0.033
	(0.025)	(0.025)	(0.024)	(0.024)
Month FE	✓	✓	✓	✓
Municipality FE	✓	✓	✓	✓
Internal mobility $\times \delta_t$	✓	✓	✓	✓
Geographic controls $\times \delta_t$	✕	✓	✓	✓
Demographic controls $\times \delta_t$	✕	✓	✓	✓
Vulnerability controls $\times \delta_t$	✕	✕	✓	✓
Economic controls $\times \delta_t$	✕	✕	✕	✓
Observations	35 916	35 916	35 916	35 916
R^2	0.08	0.09	0.10	0.11

Notes: All of the specifications present OLS estimates and include month and municipality fixed effects. Standard errors clustered at the LLM level appear in parentheses. Significance values: ***p<0.01, **p<0.05, *p<0.10.

where our commuting index is cut by 10%, 4.8% and 5.3% median reductions in mortality growth on March and April would translates into 1 346 and 997 lives saved[14] across Italy, respectively.

Finally, in Appendix A, we corroborate our empirical findings through several robustness checks, while in Appendix B, we explore the spatial heterogeneity of lockdown intensities induced by different government policies, such as the anticipation of mobility restrictions (imposed using containment areas) and the reduction of active workers (imposed using the closure of non-essential economic activities).

Section 1), would have commuting flows comparable to the provincial capital of Monza.

[14]With reference to our 7 357 municipalities, the average number of fatalities occurring in Italy at the "baseline" were 55 065 in March and 49 144 in April, while the total number of fatalities occurring during the same months in the 2020 were 82 867 (+50.5%) and 67 805 (+38.0%), respectively. According to the reductions in mortality growth for these months computed by our back-of-the-envelope calculations, the mildest scenario would have led to *mortality_growth* of 48.0% (50.5%-(50.5%*4.8%)) in March and 35.9% (38.0%-(38.0%*5.3%) in April. Hence, the "counterfactual" number of fatalities during the most critical part of the pandemic cycle would have been 81 521 in March and 66 808 in April.

Figure 4: Reduction in *mortality_growth*, by month and scenario

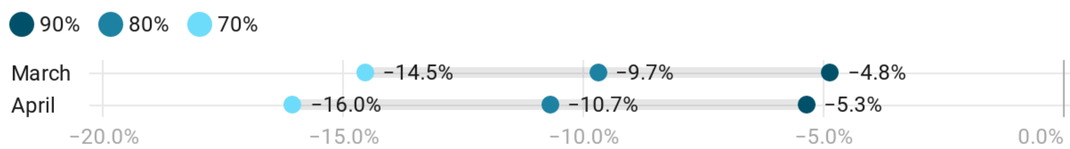

Notes: Estimates are based on back-of-the-envelope calculations along three scenarios in which the intensive margins would be equal to 90%, 80%, and 70% of those really observed in our data.

5. Conclusions

The diffusion of COVID-19 is imposing tremendous challenges on our society, and it seems that now, more than in the past few decades, geography is considered a crucial feature for resilience to such a shock. With reference to the Italian case, the virus spread first and foremost in the most industrialized area of the country, where the high density of economic activities also exhibits dense networks of commuting flows. To the best of our knowledge, this article is the first exploring the relationship between the openness of local labour markets, as defined by the structure of the commuting network, and the spread of the virus among Italian municipalities. To this end, we computed the intensive and extensive margins of commuting flows, and we measured the spread of COVID-19 by considering excess mortality over the first five months of 2020, with clear implications in terms of measurement of resilience.

Using a rich and novel dataset, we have found that, during the most critical part of the pandemic cycle (i.e., March and April 2020), municipalities with larger shares of population commuting from and to their borders for motives of labour tended to have higher COVID-19-related fatalities. Moreover, our findings also indicate that it is not only the intensity of external mobility that can influence the speed of diffusion of the virus and the depth of the shock but also the centrality of each municipality within a network of commuting flows. Indeed, municipalities strongly connected to many other different places experienced higher excess mortality in April as well. A back-of-the-envelope calculation suggests that, if structural commuting patterns were 90% of the real ones, Italy would have suffered approximately 1 300 and 1 000 fewer fatalities in March and April, respectively. The overall conclusion arising from our analysis is that places more isolated and less central in the network of commuting flows are found to be more resilient than others, all else being equal. This finding, in its turn, suggests policy actions to overcome the epidemic, considering not only the intensity of commuting flows but also their geography, which is the spatial extent of local labour markets.

Acknowledgements

We would like to thank Antonio Accetturo for comments and suggestions that substantially improved the article, as well as participants at the SIET 2020 (online). The views expressed

in this article are those of the authors and do not necessarily correspond with those of their institution. We have no conflicts of interest to disclose.

References

Alacevich, C., Cavalli, N., Giuntella, O., Lagravinese, R., Moscone, F., Nicodemo, C., 2020. Exploring the relationship between care homes and excess deaths in the COVID-19 pandemic: Evidence from Italy. IZA Discussion Paper No. 13492 .

Barbieri, T., Basso, G., Scicchitano, S., 2020. Italian workers at risk during the Covid-19 epidemic. Available at SSRN 3572065 .

Barnett, M.L., Grabowski, D.C., 2020. Nursing homes are ground zero for COVID-19 pandemic, in: JAMA Health Forum, American Medical Association. pp. e200369–e200369.

Bartoszek, K., Guidotti, E., Iacus, S.M., Okrój, M., 2020. Are official confirmed cases and fatalities counts good enough to study the COVID-19 pandemic dynamics? A critical assessment through the case of Italy. Nonlinear Dynamics .

Bartscher, A.K., Seitz, S., Slotwinski, M., Siegloch, S., Wehrhöfer, N., 2020. Social capital and the spread of Covid-19: Insights from European countries. CESifo Working Paper No. 8346 .

Becchetti, L., Conzo, G., Conzo, P., Salustri, F., 2020. Understanding the heterogeneity of adverse COVID-19 outcomes: the role of poor quality of air and lockdown decisions. Available at SSRN 3572548 .

Beria, P., Lunkar, V., 2020. Presence and mobility of the population during the first wave of Covid-19 outbreak and lockdown in Italy. Sustainable Cities and Society , 102616.

Bisin, A., Moro, A., 2020. Learning Epidemiology by Doing: The Empirical Implications of a Spatial-SIR Model with Behavioral Responses. NBER Working Paper No. 27590 .

Bonaccorsi, G., Pierri, F., Cinelli, M., Flori, A., Galeazzi, A., Porcelli, F., Schmidt, A.L., Valensise, C.M., Scala, A., Quattrociocchi, W., Pammolli, F., 2020. Economic and social consequences of human mobility restrictions under COVID-19. Proceedings of the National Academy of Sciences 117, 15530–15535.

Borgonovi, F., Andrieu, E., 2020. Bowling together by bowling alone: Social capital and Covid-19. Covid Economics 17, 73–96.

Born, B., Dietrich, A., Müller, G.J., 2020. Do lockdowns work? A counterfactual for Sweden. CEPR Discussion Paper No. DP14744 .

Borri, N., Drago, F., Santantonio, C., Sobbrio, F., 2020. The “Great Lockdown”: Inactive workers and mortality by Covid-19. CESifo Working Paper No. 8584 .

Boschma, R., 2015. Towards an evolutionary perspective on regional resilience. Regional Studies 49, 733–751.

Buonanno, P., Galletta, S., Puca, M., 2020. Estimating the severity of Covid-19: evidence from the Italian epicenter. Center for Law & Economics Working Paper Series 3.

Caselli, M., Fracasso, A., Scicchitano, S., 2020. From the lockdown to the new normal: An analysis of the limitations to individual mobility in Italy following the Covid-19 crisis. Technical Report. GLO Discussion Paper No. 2020-07.

Ciminelli, G., Garcia-Mandicó, S., 2020. Covid-19 in Italy: an analysis of death registry data. VOXEU, Centre for Economic Policy Research, London 22.

Cintia, P., Fadda, D., Giannotti, F., Pappalardo, L., Rossetti, G., Pedreschi, D., Rinzivillo, S., Bonato, P., Fabbri, F., Penone, F., et al., 2020. The relationship between human mobility and viral transmissibility during the COVID-19 epidemics in Italy. arXiv preprint arXiv:2006.03141 .

Coker, E.S., Cavalli, L., Fabrizi, E., Guastella, G., Lippo, E., Parisi, M.L., Pontarollo, N., Rizzati, M., Varacca, A., Vergalli, S., 2020. The Effects of Air Pollution on COVID-19 Related Mortality in Northern Italy. Environmental and Resource Economics , 1–24.

Conticini, E., Frediani, B., Caro, D., 2020. Can atmospheric pollution be considered a co-factor in extremely high level of SARS-CoV-2 lethality in Northern Italy? Environmental pollution , 114465.

De Vos, J., 2020. The effect of COVID-19 and subsequent social distancing on travel behavior. Transportation Research Interdisciplinary Perspectives , 100121.

Desmet, K., Wacziarg, R., 2020. Understanding Spatial Variation in COVID-19 across the United States. NBER Working Paper No. 27329 .

Di Porto, E., Naticchioni, P., Scrutinio, V., 2020. Partial lockdown and the spread of Covid-19: Lessons from the Italian case. CSEF Working Paper No. 569 .

DPCM1, 2020. Decreto del presidente del consiglio dei ministri 23 febbraio 2020 (in Italian). Retrieved 25 June 2020 from `https://www.gazzettaufficiale.it/eli/id/2020/02/23/20A01228/sg`.

DPCM2, 2020. Decreto del presidente del consiglio dei ministri 4 marzo 2020 (in Italian). Retrieved 25 June 2020 from `https://www.gazzettaufficiale.it/eli/id/2020/03/04/20A01475/sg`.

DPCM3, 2020. Decreto del presidente del consiglio dei ministri 8 marzo 2020 (in Italian). Retrieved 25 June 2020 from `https://www.gazzettaufficiale.it/eli/id/2020/03/08/20A01522/sg`.

DPCM4, 2020. Decreto del presidente del consiglio dei ministri 11 marzo 2020 (in Italian). Retrieved 25 June 2020 from https://www.gazzettaufficiale.it/eli/id/2020/03/11/20A01605/sg.

DPCM5, 2020. Decreto del presidente del consiglio dei ministri 22 marzo 2020 (in Italian). Retrieved 25 June 2020 from https://www.gazzettaufficiale.it/eli/id/2020/03/22/20A01807/sg.

DPCM6, 2020. Decreto del presidente del consiglio dei ministri 25 marzo 2020 (in Italian). Retrieved 25 June 2020 from https://www.gazzettaufficiale.it/eli/id/2020/03/26/20A01877/sg.

Durante, R., Guiso, L., Gulino, G., 2020. Asocial capital: Civic culture and social distancing during COVID-19. CEPR Discussion Paper No. DP14820 .

Fang, H., Wang, L., Yang, Y., 2020. Human mobility restrictions and the spread of the novel coronavirus (2019-nCoV) in China. NBER Working Paper No. 26906 .

Gatto, M., Bertuzzo, E., Mari, L., Miccoli, S., Carraro, L., Casagrandi, R., Rinaldo, A., 2020. Spread and dynamics of the COVID-19 epidemic in Italy: Effects of emergency containment measures. Proceedings of the National Academy of Sciences 117, 10484–10491.

Glaeser, E.L., Gorback, C.S., Redding, S.J., 2020. How much does COVID-19 Increase with Mobility? Evidence from New York and Four Other US Cities. NBER Working Paper No. 27519 .

Gordon, I.R., McCann, P., 2000. Industrial clusters: complexes, agglomeration and/or social networks? Urban studies 37, 513–532.

Greenstone, M., Nigam, V., 2020. Does social distancing matter? University of Chicago, Becker Friedman Institute for Economics Working Paper No. 2020-26 .

Haushofer, J., Metcalf, C.J.E., 2020. Which interventions work best in a pandemic? Science 368, 1063–1065.

Iacus, S.M., Santamaria, C., Sermi, F., Spyratos, S., Tarchi, D., Vespe, M., 2020. How human mobility explains the initial spread of COVID-19. Publications Office of the European Union .

INPS, 2020. Analisi della mortalità nel periodo di epidemia da covid-19 (in Italian). Retrieved 15 June 2020 from https://www.inps.it/docallegatiNP/Mig/Dati_analisi_bilanci/Nota_CGSA_mortal_Covid19_def.pdf.

ISTAT, 2020. Primi risultati dell'indagine di sieroprevalenza sul sars-cov-2 (in Italian). Retrieved 15 June 2020 from https://www.istat.it/it/files//2020/08/ReportPrimiRisultatiIndagineSiero.pdf.

Knittel, C.R., Ozaltun, B., 2020. What does and does not correlate with COVID-19 death rates. medRxiv .

Kropp, P., Schwengler, B., 2016. Three-step method for delineating functional labour market regions. Regional Studies 50, 429–445.

Lauer, S.A., Grantz, K.H., Bi, Q., Jones, F.K., Zheng, Q., Meredith, H.R., Azman, A.S., Reich, N.G., Lessler, J., 2020. The incubation period of coronavirus disease 2019 (COVID-19) from publicly reported confirmed cases: estimation and application. Annals of internal medicine 172, 577–582.

Majocchi, A., Presutti, M., 2009. Industrial clusters, entrepreneurial culture and the social environment: The effects on FDI distribution. International Business Review 18, 76–88.

Monte, F., 2020. Mobility zones. NBER Working Paper No. 27236 .

Murgante, B., Borruso, G., Balletto, G., Castiglia, P., Dettori, M., 2020. Why Italy First? Health, Geographical and Planning aspects of the Covid-19 outbreak. Sustainability 12, 5064.

OECD, 2002. Redefining Territories: The Functional Regions. OECD Publishing, Paris .

Patuelli, R., Reggiani, A., Nijkamp, P., Bade, F.J., 2009. Spatial and commuting networks, in: Complexity and spatial networks. Springer, pp. 257–271.

Patuelli, R., Reggiani, A., Nijkamp, P., Bade, F.J., 2010. The evolution of the commuting network in germany: Spatial and connectivity patterns. Journal of Transport and Land Use 2, 5–37.

Pope III, C.A., Dockery, D.W., 2006. Health effects of fine particulate air pollution: lines that connect. Journal of the air & waste management association 56, 709–742.

Porcheddu, R., Serra, C., Kelvin, D., Kelvin, N., Rubino, S., 2020. Similarity in case fatality rates (CFR) of COVID-19/SARS-COV-2 in Italy and China. The Journal of Infection in Developing Countries 14, 125–128.

Van Bavel, J.J., Baicker, K., Boggio, P.S., Capraro, V., Cichocka, A., Cikara, M., Crockett, M.J., Crum, A.J., Douglas, K.M., Druckman, J.N., et al., 2020. Using social and behavioural science to support COVID-19 pandemic response. Nature Human Behaviour , 1–12.

Zehender, G., Lai, A., Bergna, A., Meroni, L., Riva, A., Balotta, C., Tarkowski, M., Gabrieli, A., Bernacchia, D., Rusconi, S., et al., 2020. Genomic characterization and phylogenetic analysis of SARS-COV-2 in Italy. Journal of Medical Virology .

Zhou, S., Zhou, S., Liu, L., Zhang, M., Kang, M., Xiao, J., Song, T., 2019. Examining the effect of the environment and commuting flow from/to epidemic areas on the spread of Dengue Fever. International Journal of Environmental Research and Public Health 16, 5013.

Appendices

Appendix A Robustness checks

In the following appendix we briefly describe a set of robustness checks aimed at corroborating our empirical findings. First, the *intensive_margin*, which is defined as the sum of incoming and outgoing flows over the population of the area, could have some "extreme" values. Indeed, as shown in Figure 2, for 58 of 7 345 municipalities, the value of this index is greater than 1, implying that the number of workers moving from and to the municipality is greater than the number of residents. To check that these possible outliers are not affecting our results, we winsorize the *intensive_margin* by setting all of the data greater than the 99^{th} percentile to the 99^{th} percentile and all of the data less than the 1^{st} percentile to the 1^{st} percentile. By so doing, we obtain an index that takes values between 0 and 1. Accordingly, we also winsorize in the same way the *extensive_margin*. Then, we estimate Equation 4 with these new variables. As shown in Table A.1, the regression results are very consistent with the main ones provided in Table 2, indicating that these possible outliers are not driving our estimates.

Second, COVID-19 has spread dramatically in some regions and not in others. The reasons for this phenomenon are difficult to assess since they most likely depend on many factors that favour the spread of the disease through different channels. For instance, in Italy, the virus severely affected the most industrialized regions, such as Lombardy, Emilia-Romagna, Piedmont, and Veneto, which differ from the rest of the country in several characteristics. Thus, it might be relevant to verify that our previous findings are not affected by such differences among areas. To this end, we estimate Equation 4 with a more "balanced" sample by considering only the municipalities located within these four regions. The regression results provided in Table A.2 suggest that the intensity of external mobility remains a determining factor in spread of the disease in the northern regions, while there is no evidence that the topology of the network contributed as well. Our interpretation is that, within the most infected areas of the country, what matters most is the total number of workers moving between municipalities, rather than the number of different connections.

Third, despite 9-year lagged explanatory variables perhaps solving some endogeneity issues, a reasonable concern is whether the 2011 commuting flows remain informative about the current ones. As proved by Gatto et al. (2020), they are since the spatial patterns of work-related mobility seem to be remarkably preserved over such a long time interval. However, we further test the consistency over time of the commuting network by computing the intensive and extensive margins using the 2001 and 1991 official country-wide assessments of mobility for Italy. If our 2011 mobility patterns are truly "structural", we should expect similar estimates by relying on the 2001 and 1991 data. Once again, we estimate Equation 4, and the related regression results are provided in Table A.3. Clearly, the estimated coefficients are consistent with the main ones provided by Table 2, (particularly for the intensive margin), lending additional reliability to our empirical findings.

Table A.1: Commuting indices and mortality growth (winsorized variables)

	mortality_growth			
	(1)	(2)	(3)	(4)
intensive_margin × *February*	0.218*	0.219*	0.194	0.203
	(0.120)	(0.131)	(0.136)	(0.144)
intensive_margin × *March*	2.345***	2.359***	1.913***	1.940***
	(0.347)	(0.371)	(0.353)	(0.353)
intensive_margin × *April*	1.516***	1.412***	1.258***	1.317***
	(0.203)	(0.208)	(0.204)	(0.200)
intensive_margin × *May*	0.260**	0.203	0.203	0.210
	(0.122)	(0.131)	(0.141)	(0.150)
extensive_margin × *February*	-3.313**	-1.625	-1.682	-1.690
	(1.376)	(1.916)	(1.972)	(1.979)
extensive_margin × *March*	17.800	22.000*	12.560	15.900
	(11.390)	(12.600)	(11.800)	(11.090)
extensive_margin × *April*	5.868**	10.070***	4.205	5.368*
	(2.574)	(2.581)	(2.749)	(2.775)
extensive_margin × *May*	-0.544	-1.108	-2.664	-2.993
	(1.471)	(1.863)	(1.918)	(1.999)
constant	-0.034	-0.034	-0.034	-0.033
	(0.025)	(0.025)	(0.024)	(0.023)
Month FE	✓	✓	✓	✓
Municipality FE	✓	✓	✓	✓
Internal mobility × δ_t	✓	✓	✓	✓
Geographic controls × δ_t	✗	✓	✓	✓
Demographic controls × δ_t	✗	✓	✓	✓
Vulnerability controls × δ_t	✗	✗	✓	✓
Economic controls × δ_t	✗	✗	✗	✓
Observations	35 916	35 916	35 916	35 916
R^2	0.09	0.09	0.10	0.11

Notes: All of the specifications present OLS estimates and include month and municipality fixed effects. Standard errors clustered at the LLM level appear in parentheses. Significance values: ***p<0.01, **p<0.05, *p<0.10.

Table A.2: Commuting indices and mortality growth (subsample)

	mortality_growth			
	(1)	(2)	(3)	(4)
intensive_margin × *February*	-0.006	0.038	0.084	0.084
	(0.113)	(0.122)	(0.121)	(0.127)
intensive_margin × *March*	1.095**	0.762*	0.789*	0.994**
	(0.430)	(0.401)	(0.415)	(0.419)
intensive_margin × *April*	0.394*	0.326	0.471**	0.525**
	(0.207)	(0.225)	(0.232)	(0.219)
intensive_margin × *May*	-0.093	-0.052	-0.029	-0.043
	(0.127)	(0.121)	(0.123)	(0.130)
extensive_margin × *February*	-1.504	0.194	-0.883	-0.932
	(1.062)	(1.146)	(1.270)	(1.292)
extensive_margin × *March*	9.383	0.882	1.171	4.008
	(10.350)	(7.240)	(6.492)	(5.971)
extensive_margin × *April*	4.475**	2.543	-1.089	-0.722
	(2.114)	(2.027)	(2.113)	(2.129)
extensive_margin × *May*	-0.587	0.688	0.044	-0.254
	(1.001)	(1.312)	(1.482)	(1.526)
constant	-0.045	-0.045	-0.045	-0.045
	(0.047)	(0.046)	(0.045)	(0.044)
Month FE	✓	✓	✓	✓
Municipality FE	✓	✓	✓	✓
Internal mobility × δ_t	✓	✓	✓	✓
Geographic controls × δ_t	✕	✓	✓	✓
Demographic controls × δ_t	✕	✓	✓	✓
Vulnerability controls × δ_t	✕	✕	✓	✓
Economic controls × δ_t	✕	✕	✕	✓
Observations	16 451	16 451	16 451	16 451
R^2	0.14	0.15	0.16	0.16

Notes: All of the specifications present OLS estimates and include month and municipality fixed effects. Standard errors clustered at the LLM level appear in parentheses. Significance values: ***p<0.01, **p<0.05, *p<0.10.

Table A.3: Commuting indices and mortality growth (2001 and 1991 data)

	mortality_growth			
	2001 data		1991 data	
	(1)	(2)	(3)	(4)
intensive_margin × *February*	0.089	0.082	0.055	0.024
	(0.090)	(0.106)	(0.100)	(0.114)
intensive_margin × *March*	2.116***	1.488***	2.360***	1.587***
	(0.378)	(0.327)	(0.460)	(0.391)
intensive_margin × *April*	1.205***	0.880***	1.214***	0.736***
	(0.177)	(0.168)	(0.191)	(0.175)
intensive_margin × *May*	0.147	0.062	0.125	0.002
	(0.091)	(0.108)	(0.100)	(0.115)
extensive_margin × *February*	-2.227**	-0.499	-2.874**	-0.974
	(1.088)	(1.455)	(1.354)	(1.801)
extensive_margin × *March*	13.410	6.405	14.800	6.335
	(10.470)	(8.032)	(12.670)	(9.622)
extensive_margin × *April*	6.089***	3.130	5.104*	0.125
	(2.255)	(1.948)	(2.693)	(2.695)
extensive_margin × *May*	0.285	-1.788	-0.113	-2.961
	(1.143)	(1.394)	(1.482)	(1.935)
constant	-0.034	-0.034	-0.034	-0.034
	(0.026)	(0.024)	(0.026)	(0.024)
Month FE	✓	✓	✓	✓
Municipality FE	✓	✓	✓	✓
Internal mobility × δ_t	✓	✓	✓	✓
Geographic controls × δ_t	✕	✓	✕	✓
Demographic controls × δ_t	✕	✓	✕	✓
Vulnerability controls × δ_t	✕	✓	✕	✓
Economic controls × δ_t	✕	✓	✕	✓
Observations	35 916	35 916	35 916	35 916
R^2	0.08	0.10	0.08	0.10

Notes: All of the specifications present OLS estimates and include month and municipality fixed effects. Standard errors clustered at the LLM level appear in parentheses. Significance values: ***p<0.01, **p<0.05, *p<0.10.

Appendix B Spatial heterogeneity implied by different lockdown intensities

In this appendix, we provide some further evidence for the relationship between the spatial extent of local labour markets and the diffusion of the virus by exploring the spatial heterogeneity of lockdown intensities induced by two policy interventions. The first source of geographical heterogeneity is based on some municipalities being located within the first relevant "red zone" of the country, which was enforced on March 8 (DPCM3, 2020). In this area, mobility restrictions were anticipated compared to the rest of Italy; hence, it is plausible to expect that this early reduction in workers commuting played a role in flattening the mortality curve more rapidly inside the "red zone" than outside[15]. The second source of geographical heterogeneity is based on the "economic" lockdown imposed between March 22 and March 25 (DPCM5, 2020; DPCM6, 2020), which forced the closure of non-essential economic activities, as well as those with high indices of physical proximity (Barbieri et al., 2020), indicating that the different sectoral composition of economic activities among municipalities leads to different shares of inactive workers, which consequently translate into different reductions in commuting flows between areas.

B.1 The introduction of the "red zone"

We start our analysis by first considering the heterogeneity imposed by the introduction of a containment area, such as the "red zone". To this end, we first set a dummy variable (red_zone) equal to 1 if a municipality is located within the locked area, the boundaries of which are drawn in Figure B.1; then, we estimate the following augmented version of Equation 4:

$$\begin{aligned} mortality\_growth_{it} = \beta_0 &+ \theta_t intensive\_margin_i \times red\_zone_i \times \delta_t \\ &+ \omega_t extensive\_margin_i \times red\_zone_i \times \delta_t \\ &+ \beta_t intensive\_margin_i \times \delta_t + \gamma_t extensive\_margin_i \times \delta_t \\ &+ \psi_t red\_zone_i \times \delta_t + \eta_t Z_i \times \delta_t + \alpha_i + \delta_t + \epsilon_{it} \end{aligned} \tag{B.1}$$

where we add the triple interactions among; i) the intensive and extensive margins; ii) the red_zone dummy; and iii) the set of month dummies. Accordingly, the area main effects are also included.

Table B.1 reports regression results for Equation B.1. Similar to Table 2, all of the specifications include month and municipality fixed effects, while columns 1-4 progressively add our sets of control variables. We focus on the coefficients estimated by the most complete specification in column 4. Given that the "red zone" was enforced on March 8 and that the incubation time plus the confirmation time of the disease can be approximated in approximately 12 days[16],

[15] Caselli et al. (2020), providing empirical evidence that this containment area significantly lowered individual mobility.

[16] Technically, the incubation time is the time from infection until the first appearance of symptoms, while the confirmation time is the time between the first symptoms and the official confirmation of the COVID-19 case.

Figure B.1: *red_zone* enforced on March 8, 2020

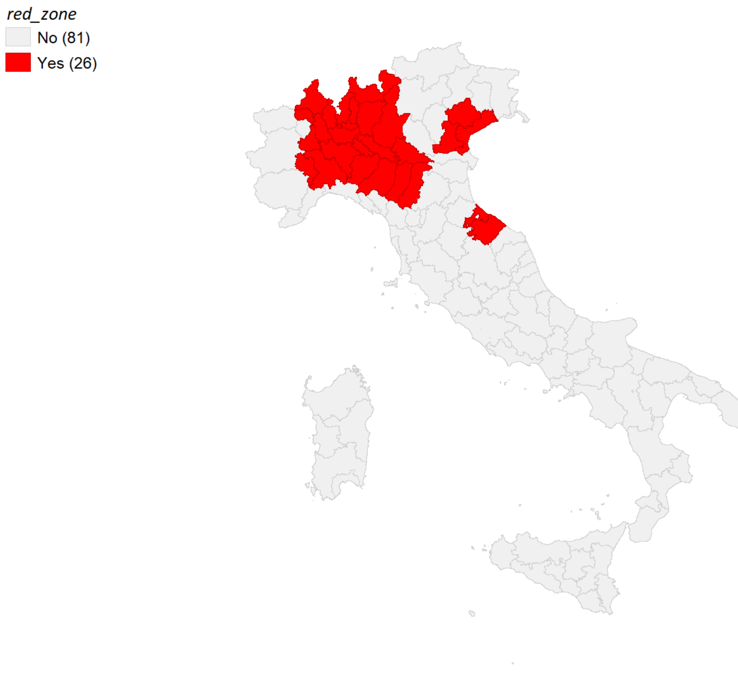

Source: Authors' own elaboration

we should observe an impact of the anticipated mobility restrictions in the area in reducing COVID-19-related fatalities from April onwards. As expected, the coefficients associated with the triple interactions involving the intensive margin in April and May are negative, but only the latter is statistically significant. This outcome suggests how an early reduction in the intensity of commuting flows, induced by an anticipated lockdown, could foster - after some weeks - a faster reduction in excess mortality related to external mobility, compared to areas without restrictions. Thus, containment areas could be useful to increase the resilience of local economies. Here, the extensive margin is not at all significant, likely because of collinearity with the *red_zone* dummy, which captures most of the variability, as shown in Figure 3. Finally, we clearly find a positive and consequently decreasing correlation between being located within the "red zone" and excess mortality. This finding confirms that the boundaries of the containment area were based on the high infection rate of the municipalities within it.

Following the WHO and the recent literature, we assume an average duration of 5 days for the incubation time (Lauer et al., 2020), while we assume an average duration of 7 days for the confirmation time (Bartscher et al., 2020).

Table B.1: Commuting indices and mortality growth (*red_zone*)

	mortality_growth			
	(1)	(2)	(3)	(4)
intensive_margin × *red_zone* × *February*	-0.143	-0.126	-0.115	-0.113
	(0.183)	(0.196)	(0.199)	(0.199)
intensive_margin × *red_zone* × *March*	0.950	0.634	0.762	0.774
	(0.618)	(0.621)	(0.610)	(0.604)
intensive_margin × *red_zone* × *April*	-0.577*	-0.525	-0.376	-0.366
	(0.323)	(0.326)	(0.332)	(0.334)
intensive_margin × *red_zone* × *May*	-0.498***	-0.463**	-0.442**	-0.439**
	(0.191)	(0.196)	(0.197)	(0.196)
extensive_margin × *red_zone* × *February*	1.571	0.728	0.478	0.481
	(1.867)	(1.899)	(1.928)	(1.929)
extensive_margin × *red_zone* × *March*	4.835	2.236	4.306	3.033
	(9.099)	(9.868)	(9.724)	(9.337)
extensive_margin × *red_zone* × *April*	3.054	2.190	3.598	3.206
	(2.892)	(3.133)	(2.838)	(2.736)
extensive_margin × *red_zone* × *May*	2.100	2.556	2.926	3.165
	(1.922)	(1.994)	(2.063)	(2.126)
intensive_margin × *February*	0.144	0.147	0.130	0.134
	(0.136)	(0.147)	(0.153)	(0.157)
intensive_margin × *March*	0.551***	0.757***	0.661***	0.764***
	(0.181)	(0.208)	(0.220)	(0.252)
intensive_margin × *April*	0.964***	0.939***	0.867***	0.923***
	(0.183)	(0.188)	(0.187)	(0.195)
intensive_margin × *May*	0.272**	0.234	0.244*	0.243
	(0.136)	(0.143)	(0.148)	(0.153)
extensive_margin × *February*	-3.171**	-1.518	-1.267	-1.365
	(1.544)	(1.772)	(1.815)	(1.832)
extensive_margin × *March*	-4.728*	-3.225	-5.602	-2.857
	(2.831)	(4.156)	(3.849)	(3.622)
extensive_margin × *April*	-1.700	-0.030	-2.787	-2.100
	(2.371)	(2.890)	(2.487)	(2.421)
extensive_margin × *May*	-1.992	-2.944	-3.814**	-4.488**
	(1.580)	(1.838)	(1.878)	(1.976)
red_zone × *February*	0.079	0.088	0.092	0.099
	(0.083)	(0.095)	(0.101)	(0.103)
red_zone × *March*	1.193***	1.425***	1.189***	1.144***
	(0.356)	(0.391)	(0.371)	(0.376)
red_zone × *April*	0.837***	0.823***	0.690***	0.691***
	(0.128)	(0.141)	(0.151)	(0.151)
red_zone × *May*	0.284***	0.265**	0.250**	0.271**
	(0.101)	(0.107)	(0.115)	(0.117)
constant	-0.033	-0.033	-0.033	-0.033
	(0.022)	(0.022)	(0.022)	(0.022)
Month FE	✓	✓	✓	✓
Municipality FE	✓	✓	✓	✓
Internal mobility × δ_t	✓	✓	✓	✓
Geographic controls × δ_t	✕	✓	✓	✓
Demographic controls × δ_t	✕	✓	✓	✓
Vulnerability controls × δ_t	✕	✕	✓	✓
Economic controls × δ_t	✕	✕	✕	✓
Observations	35 916	35 916	35 916	35 916
R^2	0.12	0.12	0.12	0.13

Notes: All of the specifications present OLS estimates and include month and municipality fixed effects. Standard errors clustered at the LLM level appear in parentheses. Significance values: ***p<0.01, **p<0.05, *p<0.10.

B.2 The introduction of the "economic" lockdown

We now turn to exploiting the variation in the share of inactive workers due to the closure of non-essential economic activities. To this end, we rely on data provided by ISTAT[17] on the number of active and inactive workers for each municipality, which are based on the list of ATECO sectors not suspended by the Italian government (see Table C.3 for a detailed list of sectors that were allowed to operate). Then, we compute our share of interest by simply dividing the number of inactive workers by the total number of workers in the area:

$$share\_inactive_i = \frac{inactive\_w_i}{w_i} \tag{B.2}$$

At this point, we are interested in understanding how much this "economic" lockdown has tightened commuting flows among municipalities, given that many workers no longer had to reach their workplaces. To do so, we compute the share of inactive commuters for each municipality in the following way:

$$share\_inactive\_commuters_i = \frac{\sum_{j=1}^{n}(w_{ij} \times share\_inactive_j + w_{ji} \times share\_inactive_i)}{\sum_{j=1}^{n}(w_{ij} + w_{ji})} \tag{B.3}$$

where the total number of workers moving from and to a municipality (as explained in Equation 2) has been first multiplied by the share of inactive workers in the municipality of destination and then weighted by the total incoming and outgoing flows. Next, we define municipalities with the largest share of inactive commuters by setting a dummy variable (*high_inactive*) that equals 1 if the value computed through Equation B.3 is greater than the 66$^{\text{th}}$ percentile. These municipalities are plotted in Figure B.2. To test whether the closure of non-essential economic activities played a role in reducing COVID-19-related fatalities by tightening commuting flows further, we estimate the following augmented version of Equation 4:

$$\begin{aligned} mortality\_growth_{it} = \beta_0 &+ \theta_t intensive\_margin_i \times high\_inactive_i \times \delta_t \\ &+ \beta_t intensive\_margin_i \times \delta_t + \gamma_t extensive\_margin_i \times \delta_t \\ &+ \psi_t high\_inactive_i \times \delta_t + \eta_t Z_i \times \delta_t + \alpha_i + \delta_t + \epsilon_{it} \end{aligned} \tag{B.4}$$

where we add the triple interaction among: i) the intensive margin; ii) the *high_inactive* dummy; and iii) the set of month dummies. Accordingly, the area main effects are included. Note that we do not add the triple interaction involving the extensive margin because the closure

[17] Data are retrieved from `https://www.istat.it/it/archivio/241341`. For the sake of clarity, ISTAT data (which are based on the 2017 *Frame Territoriale* register) focus on workers in the industrial and service sectors. Workers employed in other economic activities, such as agriculture and public administration, are excluded from the registry because these sectors are outside the scope of business statistics.

Figure B.2: *share_inactive_commuters*, by municipality

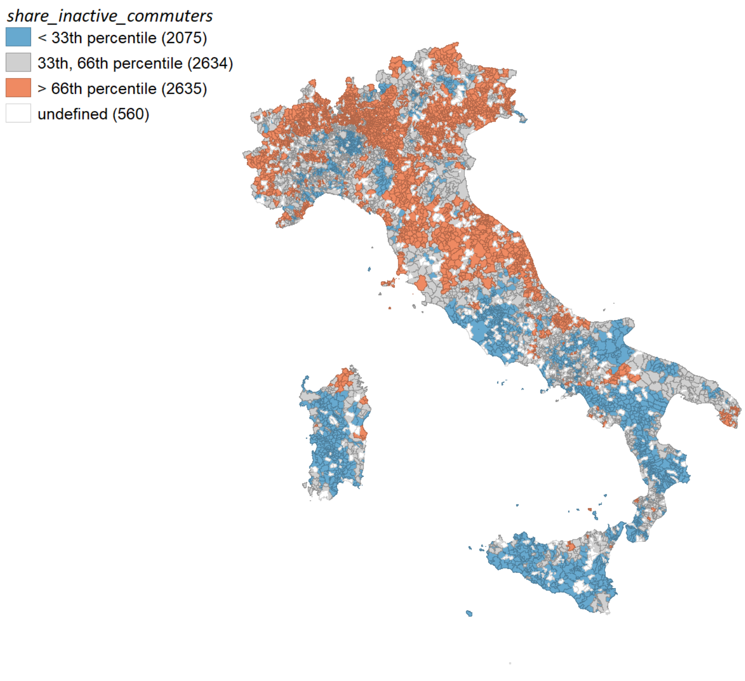

Source: Authors' own elaboration

of non-essential economic activities affected the intensity of commuting flows, rather than the number of connections between municipalities.

Table B.2 reports regression results for Equation B.4. Different from the previous tables, column 1 directly reports the estimated coefficients for the most complete specification. Here, the negative and significant coefficient associated with the triple interaction in April suggests that municipalities with the largest share of inactive commuters would benefit from a faster reduction in excess mortality. Interestingly, this finding is in line with the recent empirical evidence provided by Borri et al. (2020) and Di Porto et al. (2020). In columns 2 and 3, we further examined this point by splitting the sample between municipalities located inside and outside the "red zone". The rationale for the sample split is testing whether this second policy made an additional contribution to reducing COVID-19-related fatalities - through a further restriction of workers commuting - even within an area that had already been affected by the first policy. As it is plausible to expect, the effectiveness of the "economic" lockdown in reducing commuting flows further (and therefore in better controlling virus transmissions) lessened within the "red zone". In fact, the coefficients associated with the triple interactions are nowhere significant in column 2. Conversely, the coefficients retain their magnitudes and significance in column 3, indicating that the national dynamics also hold outside the "red zone". Accordingly, the same explanation applies.

Table B.2: Commuting indices and mortality growth (*high_inactive*)

	mortality_growth		
	Italy	inside *red_zone*	outside *red_zone*
	(1)	(2)	(3)
$intensive\_margin \times high\_inactive \times February$	0.144	0.003	0.222
	(0.192)	(0.303)	(0.305)
$intensive\_margin \times high\_inactive \times March$	-0.084	0.202	-0.012
	(0.572)	(1.031)	(0.504)
$intensive\_margin \times high\_inactive \times April$	-0.651**	-0.457	-0.866**
	(0.296)	(0.547)	(0.342)
$intensive\_margin \times high\_inactive \times May$	-0.165	0.076	-0.318
	(0.198)	(0.345)	(0.301)
$intensive\_margin \times February$	0.045	0.055	0.092
	(0.126)	(0.202)	(0.183)
$intensive\_margin \times March$	1.391***	1.239**	0.733***
	(0.324)	(0.608)	(0.189)
$intensive\_margin \times April$	1.164***	0.826*	1.304***
	(0.241)	(0.488)	(0.247)
$intensive\_margin \times May$	0.167	-0.199	0.402**
	(0.139)	(0.229)	(0.188)
$extensive\_margin \times February$	-0.669	-0.861	-1.758
	(1.120)	(1.399)	(2.133)
$extensive\_margin \times March$	8.769	-0.491	-3.408
	(6.550)	(6.226)	(2.431)
$extensive\_margin \times April$	2.978*	-4.992**	-0.078
	(1.657)	(2.387)	(2.380)
$extensive\_margin \times May$	-1.765	-1.372	-4.751**
	(1.130)	(1.786)	(1.954)
$high\_inactive \times February$	-0.057	0.025	-0.095
	(0.0856)	(0.158)	(0.117)
$high\_inactive \times March$	0.213	0.086	-0.027
	(0.248)	(0.557)	(0.191)
$high\_inactive \times April$	0.225**	0.242	0.177
	(0.113)	(0.266)	(0.138)
$high\_inactive \times May$	0.041	-0.005	0.034
	(0.091)	(0.196)	(0.119)
constant	-0.033	-0.035	-0.032**
	(0.024)	(0.053)	(0.015)
Month FE	✓	✓	✓
Municipality FE	✓	✓	✓
Internal mobility × δ_t	✓	✓	✓
Geographic controls × δ_t	✓	✓	✓
Demographic controls × δ_t	✓	✓	✓
Vulnerability controls × δ_t	✓	✓	✓
Economic controls × δ_t	✓	✓	✓
Observations	35 911	11 869	24 042
R^2	0.11	0.22	0.03

Notes: All of the specifications present OLS estimates and include month and municipality fixed effects. Standard errors clustered at the LLM level appear in parentheses. Significance values: ***p<0.01, **p<0.05, *p<0.10.

Appendix C Additional Tables

Table C.1: Descriptive statistics

	Mean	SD	Minimum	Maximum	Observations	Year[a]
mortality_growth	0.313	1.540	-1.000	39.000	35 916	2020
intensive_margin	0.334	0.189	0.000	3.898	36 725	2011
extensive_margin	0.012	0.013	0.000	0.339	36 725	2011
internal_mobility	0.114	0.053	0.000	0.403	36 725	2011
coastal	0.078	0.268	0.000	1.000	36 725	2011
mountainous	0.732	0.443	0.000	1.000	36 725	2011
ln_density	4.718	1.406	-0.266	9.411	36 725	2019
$ln\_house\_m^2\_pc$	3.763	0.134	3.266	4.450	36 725	2011
share_males	0.496	0.017	0.414	0.650	36 725	2019
$share\_over75$	0.119	0.042	0.025	0.435	36 725	2011
$share\_cohab\_over65$	0.360	0.124	0.075	1.781	36 725	2011
hospital_beds_pc	0.004	0.001	0.000	0.007	36 725	2017
$pm10$	29.678	8.746	14.000	46.000	36 725	2017
district	0.265	0.441	0.000	1.000	36 725	2011
remote_working	0.471	0.019	0.384	0.609	36 725	2011

[a] Note that the number of Italian municipalities decreased from 8 092 in 2011 to 7 904 in 2020. Hence, we precisely combined data by considering all of the administrative variations occurring in Italy during these 9 years, such as the establishment of new municipalities and the suppression of others. Considering that *mortality_growth* data are available for 7 357 municipalities, we ended up with 7 345 observations for each month.

Table C.2: Commuting indices and mortality growth (part 3)

	mortality_growth			
	(1)	(2)	(3)	(4)
intensive_margin × *February*	0.114	0.120	0.096	0.098
	(0.095)	(0.102)	(0.103)	(0.108)
intensive_margin × *March*	1.896***	1.804***	1.430***	1.427***
	(0.299)	(0.292)	(0.285)	(0.277)
intensive_margin × *April*	1.141***	1.034***	0.882***	0.906***
	(0.170)	(0.173)	(0.166)	(0.162)
intensive_margin × *May*	0.153	0.107	0.095	0.095
	(0.094)	(0.099)	(0.104)	(0.108)
extensive_margin × *February*	-1.881**	-0.698	-0.748	-0.771
	(0.891)	(1.075)	(1.086)	(1.093)
extensive_margin × *March*	14.000	11.820	6.064	8.556
	(8.531)	(7.995)	(6.930)	(6.596)
extensive_margin × *April*	6.032***	6.263***	2.643*	3.442**
	(1.767)	(1.680)	(1.567)	(1.590)
extensive_margin × *May*	0.198	-0.405	-1.352	-1.620
	(0.926)	(1.026)	(1.054)	(1.109)
internal_mobility × *February*	0.412	0.406	0.472	0.484
	(0.318)	(0.342)	(0.346)	(0.367)
internal_mobility × *March*	-2.033	-1.700	-0.042	-0.483
	(1.299)	(1.288)	(1.129)	(1.206)
internal_mobility × *April*	-0.584	-0.205	0.473	0.396
	(0.513)	(0.506)	(0.520)	(0.531)
internal_mobility × *May*	-0.049	0.154	0.215	0.265
	(0.349)	(0.357)	(0.361)	(0.381)
coastal × *February*		-0.065	-0.060	-0.062
		(0.047)	(0.049)	(0.051)
coastal × *March*		-0.398***	-0.215**	-0.182**
		(0.106)	(0.100)	(0.091)
coastal × *April*		-0.228***	-0.155**	-0.157**
		(0.063)	(0.065)	(0.073)
coastal × *May*		-0.085*	-0.061	-0.064
		(0.048)	(0.049)	(0.051)
mountainous × *February*		0.027	0.028	0.027
		(0.034)	(0.037)	(0.037)
mountainous × *March*		-0.281	-0.073	-0.073
		(0.177)	(0.167)	(0.167)
mountainous × *April*		-0.064	-0.002	-0.005
		(0.080)	(0.076)	(0.076)
mountainous × *May*		0.046	0.051	0.0513
		(0.040)	(0.044)	(0.043)
ln_density × *February*		-0.014	0.003	0.004
		(0.020)	(0.022)	(0.022)
ln_density × *March*		-0.035	-0.056	-0.057
		(0.059)	(0.066)	(0.060)
ln_density × *April*		-0.001	-0.018	-0.014
		(0.030)	(0.035)	(0.038)
ln_density × *May*		0.026	0.018	0.018
		(0.020)	(0.021)	(0.022)
ln_house_m^2_pc × *February*		-0.018	0.007	0.011
		(0.149)	(0.169)	(0.171)
ln_house_m^2_pc × *March*		-0.636	-1.428**	-1.561***
		(0.490)	(0.581)	(0.572)
ln_house_m^2_pc × *April*		0.476*	-0.063	-0.082
		(0.243)	(0.291)	(0.299)
ln_house_m^2_pc × *May*		0.239	0.087	0.010

Continued on next page

Table C.2 – continued from previous page

	mortality_growth			
	(1)	(2)	(3)	(4)
		(0.183)	(0.196)	(0.202)
share_males × *February*			2.425	2.420
			(1.631)	(1.649)
share_males × *March*			8.683***	7.528***
			(2.969)	(2.621)
share_males × *April*			-1.242	-1.605
			(1.888)	(1.851)
share_males × *May*			-2.777*	-2.658*
			(1.480)	(1.479)
share_over75 × *February*			0.361	0.385
			(1.855)	(1.879)
share_over75 × *March*			-0.789	-0.301
			(3.609)	(3.533)
share_over75 × *April*			-3.932	-3.759
			(2.607)	(2.595)
share_over75 × *May*			0.396	0.306
			(1.944)	(1.952)
share_cohab_over65 × *February*			-0.058	-0.070
			(0.673)	(0.680)
share_cohab_over65 × *March*			0.531	0.485
			(1.195)	(1.181)
share_cohab_over65 × *April*			1.737*	1.714*
			(0.949)	(0.950)
share_cohab_over65 × *May*			0.006	0.016
			(0.709)	(0.717)
hospital_beds_pc × *February*			20.600	20.320
			(21.620)	(21.680)
hospital_beds_pc × *March*			-43.860	-44.200
			(64.560)	(66.320)
hospital_beds_pc × *April*			60.520**	60.000**
			(30.090)	(30.230)
hospital_beds_pc × *May*			31.110	30.830
			(24.050)	(24.130)
pm10 × *February*			-0.001	-0.001
			(0.003)	(0.003)
pm10 × *March*			0.054***	0.049***
			(0.012)	(0.011)
pm10 × *April*			0.022***	0.021***
			(0.005)	(0.005)
pm10 × *May*			0.005*	0.005*
			(0.003)	(0.003)
district × *February*				-0.010
				(0.045)
district × *March*				0.531*
				(0.280)
district × *April*				0.133
				(0.093)
district × *May*				-0.053
				(0.049)
remote_working × *February*				-0.038
				(1.339)
remote_working × *March*				-8.424***
				(2.750)
remote_working × *April*				-3.301*
				(1.959)
remote_working × *May*				0.876

Continued on next page

Table C.2 – continued from previous page

	mortality_growth			
	(1)	(2)	(3)	(4)
				(1.370)
constant	-0.034	-0.034	-0.034	-0.033
	(0.025)	(0.025)	(0.024)	(0.024)
Month FE	✓	✓	✓	✓
Municipality FE	✓	✓	✓	✓
Observations	35 916	35 916	35 916	35 916
R^2	0.08	0.09	0.10	0.11

Notes: All of the specifications present OLS estimates and include month and municipality fixed effects. Standard errors clustered at the LLM level appear in parentheses. Significance values: ***p<0.01, **p<0.05, *p<0.10.

Table C.3: ATECO sectors allowed to operate during the "economic" lockdown

ATECO		Description
Section	Code	
A: Agriculture	01	Crop and animal production
	03	Fishing and aquaculture
B: Mining	05	Mining of coal and lignite
	06	Extraction of crude petroleum and natural gas
	09.1	Support activities for petroleum and natural gas extraction
C: Manufacturing	10	Manufacture of food products
	11	Manufacture of beverages
	13.95	Manufacture of non-wovens and articles made from non-wovens, except apparel
	13.96	Manufacture of other technical and industrial textiles
	14.12	Manufacture of workwear
	16.24	Manufacture of wooden containers
	17	Manufacture of paper and paper products
	18	Printing and reproduction of recorded media
	19	Manufacture of coke and refined petroleum products
	20	Manufacture of chemicals and chemical products
	21	Manufacture of basic pharmaceutical products and pharmaceutical preparations
	22.2	Manufacture of plastic products
	23.13	Manufacture of hollow glass
	23.19	Manufacture and processing of other glass, including technical glassware
	25.21	Manufacture of central heating radiators and boilers
	25.92	Manufacture of light metal packaging
	26.6	Manufacture of irradiation, electromedical and electrotherapeutic equipment
	27.1	Manufacture of electric motors, generators, transformers and electricity distribution
	27.2	Manufacture of batteries and accumulators
	28.29	Manufacture of other general-purpose machinery n.e.c.[a]
	28.95	Manufacture of machinery for paper and paperboard production
	28.96	Manufacture of plastic and rubber machinery
	32.50	Manufacture of medical and dental instruments and supplies
	32.99	Other manufacturing n.e.c.[a]
	33	Repair and installation of machinery and equipment
D: Energy, Gas	35	Electricity, gas, steam and air conditioning supply
E: Water, Waste	36	Water collection, treatment and supply
	37	Sewerage
	38	Waste collection, treatment and disposal activities; materials recovery
	39	Remediation activities and other waste management services
F: Construction	42	Civil engineering
	43.2	Electrical, plumbing and other construction installation activities
G: Trade	45.2	Maintenance and repair of motor vehicles
	45.3	Sale of motor vehicle parts and accessories
	45.4	Sale, maintenance and repair of motorcycles and related parts and accessories
	46.2	Wholesale of agricultural raw materials and live animals

Continued on next page

Table C.3 – continued from previous page

ATECO		Description
Section	Code	
	46.3	Wholesale of food, beverages and tobacco
	46.46	Wholesale of pharmaceutical goods
	46.49	Wholesale of other household goods
	46.61	Wholesale of agricultural machinery, equipment and supplies
	46.69	Wholesale of other machinery and equipment
	46.71	Wholesale of solid, liquid and gaseous fuels and related products
H: Transportation	49	Land transport and transport via pipelines
	50	Water transport
	51	Air transport
	52	Warehousing and support activities for transportation
	53	Postal and courier activities
I: Accommodation	55.1	Hotels and similar accommodations
J: Information	58	Publishing activities
	59	Motion picture, video and television programme production and sound recording
	60	Programming and broadcasting activities
	61	Telecommunications
	62	Computer programming, consultancy and related activities
	63	Information service activities
K: Finance, Insurance	64	Financial service activities, except insurance and pension funding
	65	Insurance, reinsurance and pension funding, except compulsory social security
	66	Activities auxiliary to financial services and insurance activities
M: Professional services	69	Legal and accounting activities
	70	Activities of head offices; management consultancy activities
	71	Architectural and engineering activities; technical testing and analysis
	72	Scientific research and development
	74	Other professional, scientific and technical activities
	75	Veterinary activities
N: Other services	78.2	Temporary employment agency activities
	80.1	Private security activities
	80.2	Security systems service activities
	81.2	Cleaning activities
	82.20	Activities of call centres
	82.92	Packaging activities
	82.99	Other business support service activities n.e.c.[a]
O: Public administration	84	Public administration and defence; compulsory social security
P: Education	85	Education
Q: Health	86	Human health activities
	87	Residential care activities
	88	Social work activities without accommodations
S: Other activities	94	Activities of membership organizations
	95.11	Repair of computers and peripheral equipment

Continued on next page

Table C.3 – continued from previous page

ATECO		Description
Section	Code	
	95.12	Repair of communication equipment
	95.22	Repair of household appliances and home and garden equipment
T: Household activities	97	Activities of households as employers of domestic personnel

[a] Not elsewhere classified.

Notes: We refer to the revised list of ATECO sectors provided by the Italian government on March 25 (DPCM6, 2020), which integrated the previous list provided on March 22 (DPCM5, 2020). Some of the ATECO categories are specified also at the 5-digit level. For simplicity, we consider as active any 4-digit ATECO sector embedding the 5-digit one.

Appendix D Additional Figures

Figure D.1: Evolution of *mortality_growth* in Italy, January-May 2020

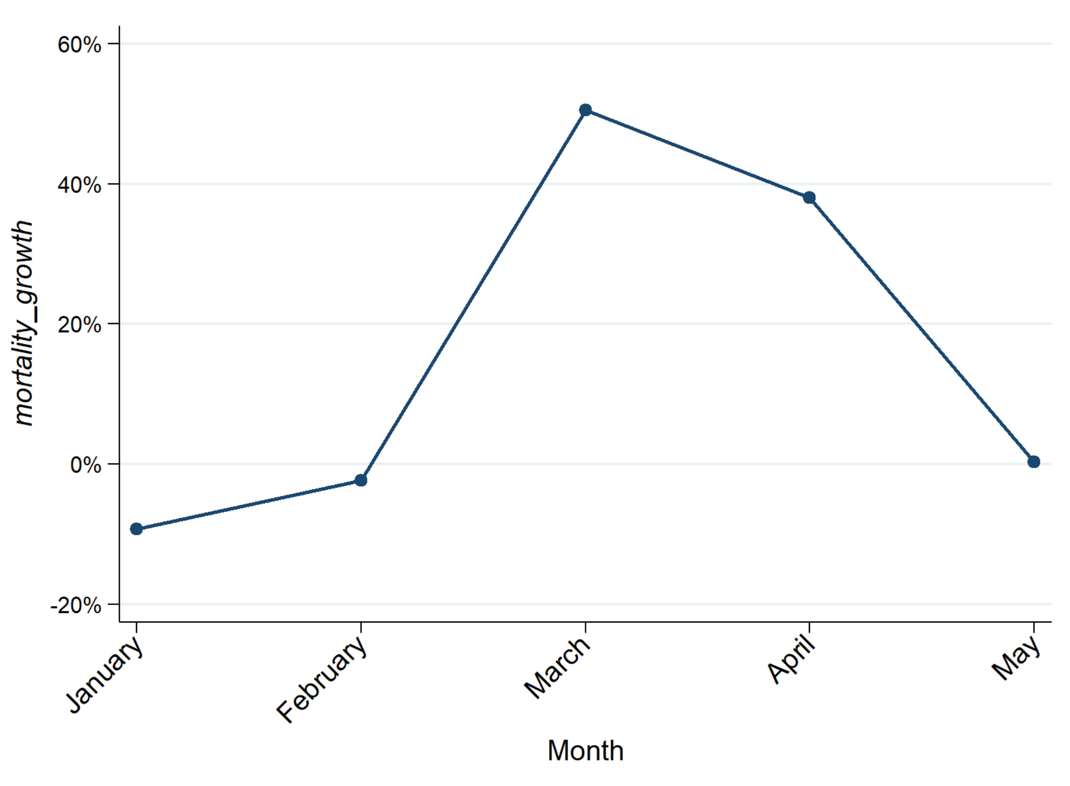

Notes: The figure plots the evolution of excess mortality in Italy during the period of analysis. It points out how the containment measures adopted in March 2020 were essential in flattening the curve since *mortality_growth* was reduced to almost the pre-pandemic level by May. *Source*: Authors' own elaboration

Figure D.2: *mortality_growth*, by month and municipality

(a) January

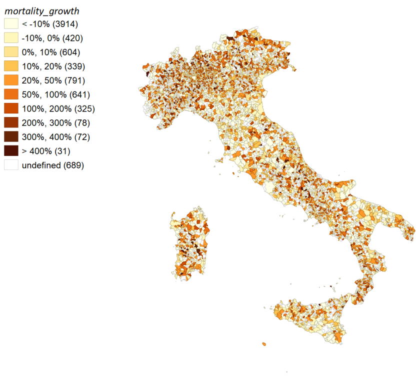

(b) February

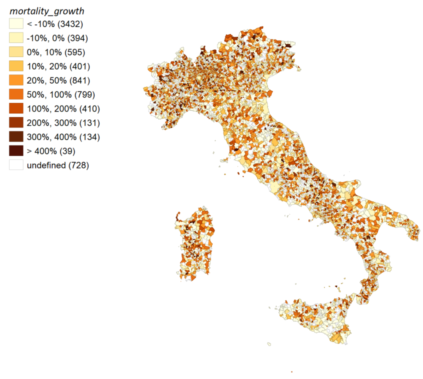

(c) March

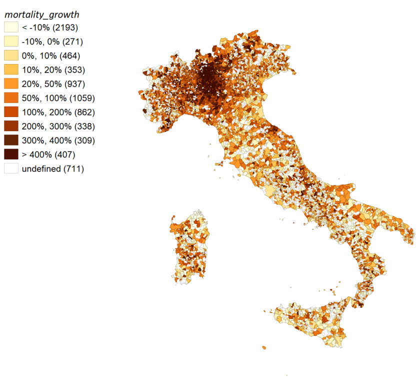

(d) April

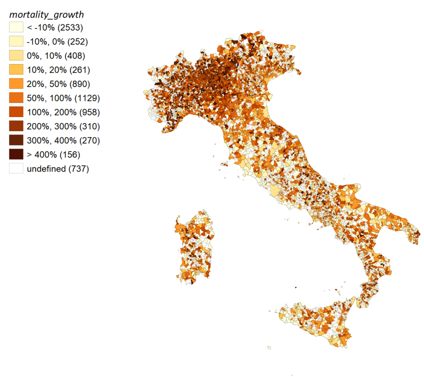

(e) May

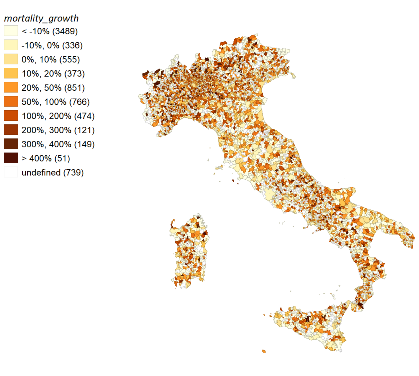

Source: Authors' own elaboration

Figure D.3: Control variables, by municipality

(a) *internal_mobility*

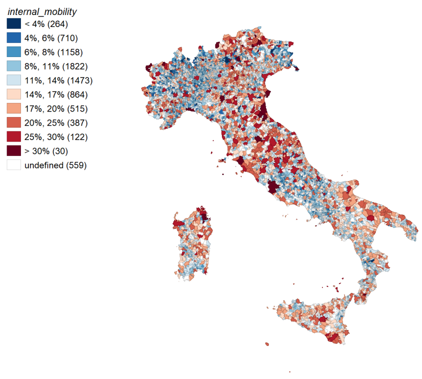

(b) *share_over*75

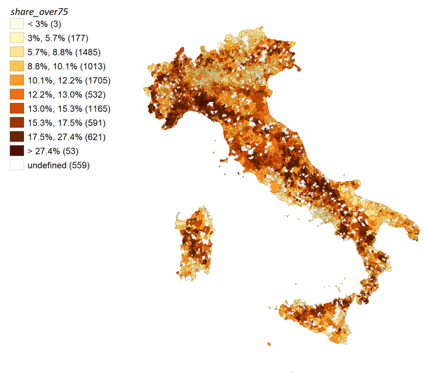

(c) *hospital_beds_pc*

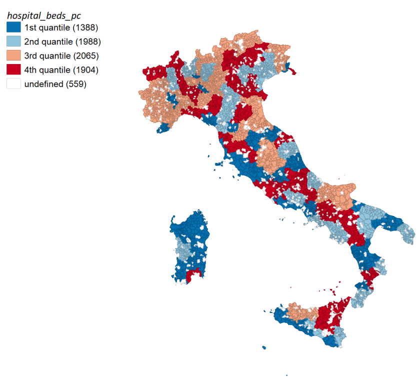

(d) *pm*10

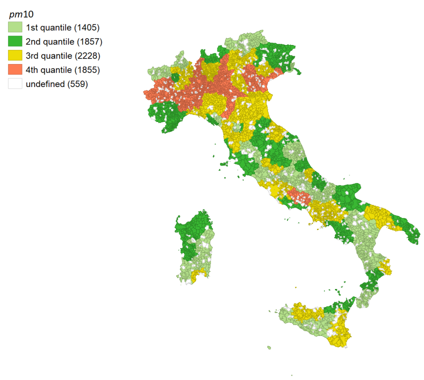

(e) *district*

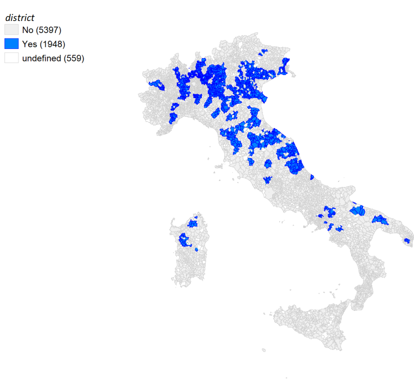

(f) *remote_working*

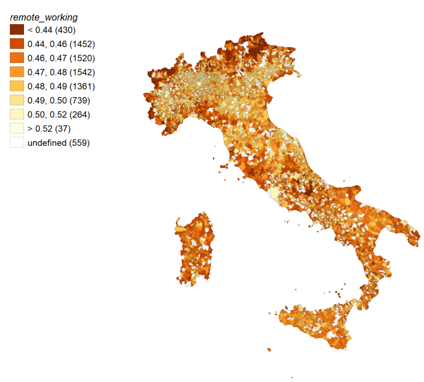

Source: Authors' own elaboration

Figure D.4: Estimated coefficients of the commuting indices, by month

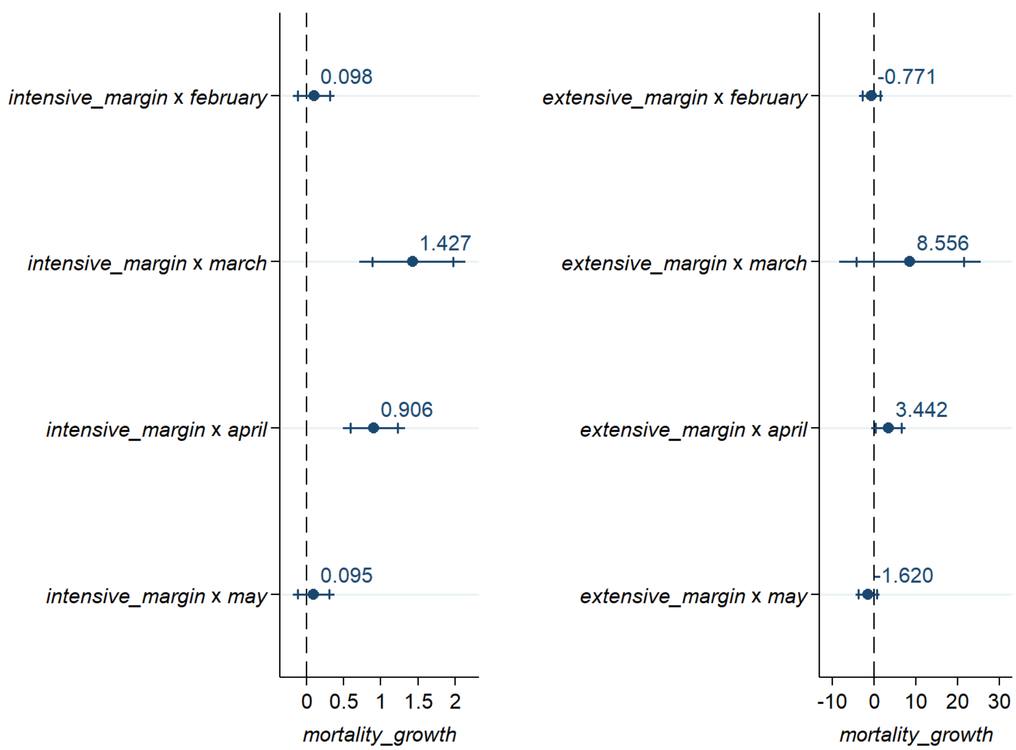

Notes: The figure plots the coefficients of the specification in column 4 of Table 2. Horizontal bands represent ± 1.96 and ± 2.58 times the standard error of each point estimate. The figure clearly shows the decreasing trend over time in the magnitude of all coefficients from March onwards, suggesting how the lockdown was crucial in reducing excess mortality. *Source*: Authors' own elaboration.

GREEN
Centre for Geography, Resources, Environment, Energy and Networks
via Röntgen, 1
20136 Milano - Italia

www.green.unibocconi.eu